Behavior of Foundation Piles for Offshore Wind Energy Plants under Axial Cyclic Loading

K. Abdel-Rahman, M. Achmus

Institute of Soil Mechanics, Foundation Engineering and Waterpower Engineering
Leibniz University of Hannover, Germany

Abstract: Offshore wind energy plants promise to become an important source of energy in the near future. It is expected that within 10 years, wind parks with a total capacity of thousands of megawatts will be installed in European seas. The foundation of such offshore wind energy plants plays an important role in the stability of these structures. High demands have to be made concerning foundation design and construction methods to find economical and technically optimal solutions. Two foundation concepts which will be used in this field are the jacket and the tripod. Under the wind and waves action, the piles will be subjected to highly cyclic tension or compressive loading. Regarding design practice and research in the field of the soil-structure-interaction the behavior of these foundations could be covered using numerical modeling. A two-dimensional numerical model using the finite element system ABAQUS will be developed. In this model the material behavior of the subsoil is described using an elasto-plastic constitutive model with Mohr-Coulomb failure criterion. A new approach based on cyclic shear deformation along the pile was implemented in ABAQUS to simulate numerically the behaviour of tension piles under cyclic loading. Preliminary results are presented concerning the capacity of piles under cyclic axial loading.

Keywords: Offshore, Tripod, Jacket, soil-structure-interaction, Abaqus, Mohr-Coulomb, cyclic loading, skin friction degradation.

1. Introduction

Many offshore structures are constructed using deep piled foundations (e.g. tripod & jacket) in order to transfer structural dead load to the ground. For example, the tripod foundation system consists of a spatial steel frame transferring the forces from the tower to primarily tension and compression forces in three hollow steel piles driven into the seabed, located in the corners of a triangle (see Figure 1). The planned plants are to have hub heights of approximately 100 m and rotor diameters of approximately 120 m.

The behavior of these piles acting in compression has been widely studied using numerical modeling, centrifuge modeling and full-scale testing. Upwards tensile loads may however be applied to these piles owing to the action of horizontal wind or wave forces on the offshore structure and the behavior of the piles under these loads is not well documented. Cyclic behavior of axially loaded piles has been an issue since studies revealed that the capability of transferring skin friction into the ground is highly dependent on the level and the number of load cycles. In this paper, the behavior of tension piles under cyclic loading using the techniques of finite element

analysis will be described, and their results will be evaluated to give an insight into the behavior of tension piles under axial cyclic loading.

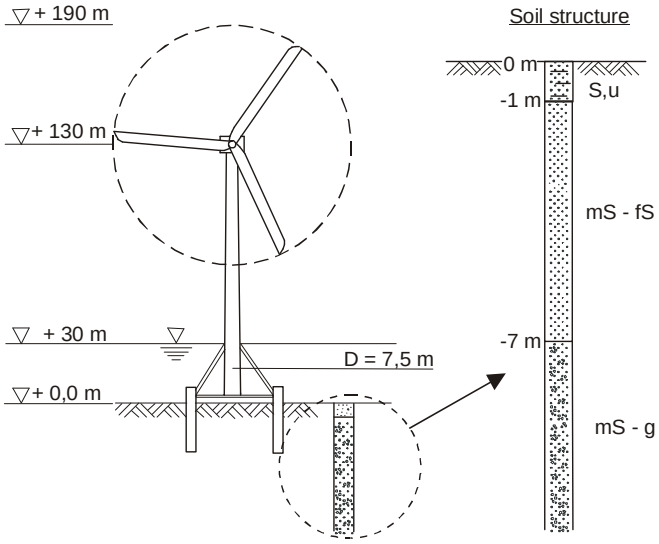

Figure 1. Example of a tripod foundation

2. Overview of previous work

Under cyclic axial loads, degradation of ultimate skin friction and with that a decrease of the pile capacity is to be expected. Different studies on steel pipe piles in non-cohesive soils have been carried out. Some investigations were made at a test field in Dunkirk under the supervision of the Imperial College in London (Jardine & Standing, (2000)). It has been shown that degradation of skin friction due to axial cyclic loading leads to accumulating displacements and a severe reduction in pile capacity.

Due to experience, no pile capacity reduction is to be expected if a certain magnitude of the cyclic load portion is not exceeded. The threshold value is termed the critical level of repeated loading (CLRL):

$$CLRL = \frac{E_{cycl}}{R_k} \tag{1}$$

Here E_{cycl} is the cyclic load amplitude and R_k is the static pile capacity. From an evaluation of literature results, Schwarz (2002) reported the *CLRL*-values given in Table 1. The table shows clearly that piles in non-cohesive soils are more sensitive to cyclic axial loading than piles in cohesive soils.

Table 1. Critical level of repeated loading according to Schwarz (2002)

Soil type	*CLRL*
Sand	0.1 – 0.4
Silt	0.4 – 0.6
Clay, normally consolidated	0.3 – 0.55
Clay, overconsolidated	0.85 – 1.0

Poulos (1988) presented a cyclic stability diagram for axially loaded piles. Based on several model and field tests, the load cycle numbers leading to pile failure are given dependent on the normalized mean load E_0/R_k and the cyclic load amplitude E_{cycl}/R_k. A "stable" region is defined here with $E_{cycl}/R_k \leq 0.2$ (i.e. $CLRL = 0.2$) for $E_0 \leq 0.6\ R_k$.

Kempfert (2009) evaluated pile test results in cohesive and non-cohesive soils separately and proposed the following approach to determine the critical cyclic load amplitude:

$$\frac{E_{cycl}}{R_k} \leq \kappa^* \cdot \left(1 - \left(\frac{E_0}{R_k} + 0.65 - \kappa^*\right)^4\right) \tag{2}$$

The factor κ^* is dependent on the number of load cycles and the type of soil and is given in the following table:

Table 2. κ *-value dependent on the number of load cycles and soil type (Kempfert 2009)

Number of load cycles N	10^1	10^2	10^3	10^4	10^5	10^6
κ^* non-cohesive	0.43	0.38	0.33	0.28	0.23	0.18
κ^* cohesive	0.48	0.43	0.38	0.33	0.28	0.23

It is generally assumed that the reason for the decrease of skin friction is the compaction of the sand directly beneath the pile shaft due to cyclic shearing. According to Randolph (2009), who evaluated cyclic interface tests on sand, the soil compaction occurs mainly within a small shear band around the pile. In a model proposed by Richter & Kirsch (2010), compaction occurs up to a distance at which a threshold value of cyclic shear strain in the soil is reached. The latter model is used for the numerical approach and is described more detailed below.

3. Description of the proposed approach

Richter & Kirsch (2010) developed a calculation method for the decrease of ultimate skin friction on cyclic axially loaded piles. In a first step, the distribution of shear stresses along the pile under the cyclic load portion has to be determined. At a certain depth, the attenuation of shear stresses τ with increasing distance r from the pile axis is described by following equation:

$$\tau(r) = \tau \cdot \frac{r_0}{r} = \gamma(r) \cdot \tilde{G} \tag{3}$$

Here r_0 is the pile radius. A cyclic shear modulus, which can be calculated from the maximum shear modulus as a function of cyclic shear strain, is used to calculate the cyclic shear strain amplitude.
The compaction effect on a soil sample due to application of 10 cycles of shear strain was investigated previously by Silver & Seed (1971) by performing cyclic simple shear tests on sand. Their results can be presented as a relationship between the volume reduction due to compaction (ε_{ii}) and the cyclic shear strain (see Fig. 2). Richter & Kirsch assumed a logarithmic dependence of volume compaction and number of cycles and thus extended the equation by introducing $\log_{10}N$:

$$\varepsilon_{ii} = 0.5 \cdot \left(\tilde{\gamma} - \alpha.\gamma_{lim}\right) \cdot I_d^{-2.32} \cdot log_{10}N \tag{4}$$

Here I_d is the relative density of the sand specimen. By integrating the volumetric strain due to compaction (ε_{ii}), a radial displacement u_r can be calculated. The integration is carried out up to a limiting distance r_{limit}, at which the cyclic strain amplitude becomes smaller than a threshold value γ_{lim}. This threshold value γ_{lim} can be derived from Vucetic (1994).

For non-cohesive soil, γ_{lim} can be set to 0.01%. The factor α in the Eq. (4) is a parameter introduced by Richter & Kirsch (2010), which can be derived from cyclic simple shear test. From Silver & Seed's results a value of $5 \cdot 10^{-5}$ for ($\alpha\ \gamma_{lim}$) can be calculated, which leads to α=0.5. Interpreting u_r as an expansion of the pile diameter and applying the elastic solution of cavity expansion problem, the corresponding change of radial soil stress ($\Delta\sigma_r$) and of skin friction ($\Delta\tau$) can be calculated:

$$\Delta\tau(N) = 2 \cdot G_w \cdot \tan\delta \cdot \Delta D^* \cdot \left[\tilde{\gamma} \cdot \left(\frac{\tilde{\gamma}}{\gamma_{limit}} - 1\right) - \frac{1}{2} \cdot \alpha \cdot \gamma_{limit} \left[\left(\frac{\tilde{\gamma}}{\gamma_{limit}}\right)^2 - 1\right]\right] \tag{5a}$$

$$\Delta D^* = \Delta D \cdot \log_{10} N = 0.5 \cdot I_D^{-2.32} \cdot \log_{10} N \tag{5b}$$

Here G_w is the reloading shear modulus of the soil. For more details refer to Richter & Kirsch (2010).

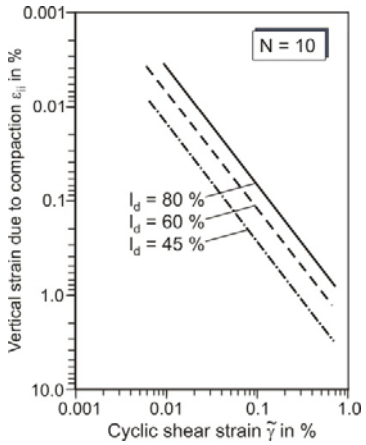

Figure 2. Cyclic vertical compaction of sand after 10 cycles (Silver & Seed 1971)

4. Numerical Modeling

In the numerical approach, the basic idea of Richter & Kirsch is adopted by using Eq. (4) to determine volumetric compaction of the soil induced by cyclic shear strain. However, the shear stress and shear strain distributions in the soil beneath the pile and also the stress changes due to the volumetric compaction are calculated by means of a finite element model of the pile-soil system. The computations were carried out using the finite element program system ABAQUS (Abaqus 2010).

4.1 Mesh Design

A two-dimensional (2D-axisymmetric) finite element model to investigate the axial deformation response of a pile in sandy soil in this study was established. The finite element mesh used in the analysis is shown in Fig. 3. The elements used to model the soil are 4-noded axisymmetric elements. The elements are biased towards the pile in order to give most data in the region of greatest interest, i.e. close to the pile. The limits of the mesh were at a radius of 25.0m and 15.0m below the base of the pile, it was verified that with model dimensions used the calculated behavior of the pile is not affected by the boundary conditions.

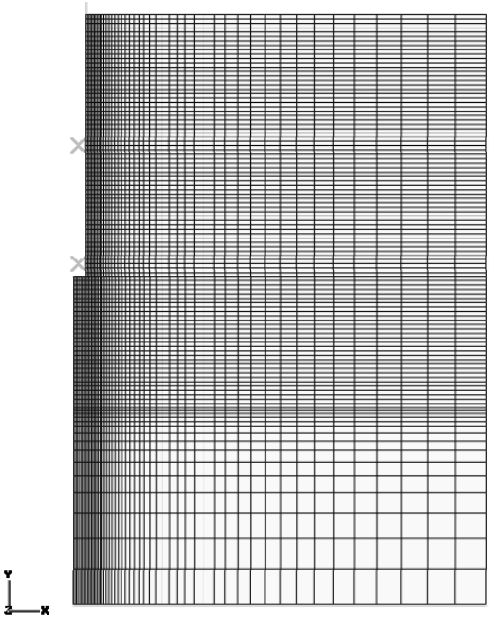

Figure 3. Finite element mesh

The piles were assumed to be rigid (non-deformable) and were modeled using "rigid body" option in ABAQUS and the displacements were controlled by referring to reference nodes of the rigid body. Different pile dimensions (diameter & length) were used in order to perform a parametric study to examine the overall behavior of tension piles. Three different piles diameters (D=2.0m, 2.50m & 3.0m) and three different embedded lengths (L=20.0m, 25.0m, & 30.0m) were modeled.

4.2 Constitutive Model

To account for the non-linear soil behavior, soil elements were simulated as elasto-plastic material with Mohr-Coulomb failure criterion. A stress dependency of the oedometric stiffness modulus was implemented as follows:

$$E_s = \kappa\, \sigma_{at} \left(\frac{\sigma_m}{\sigma_{at}}\right)^{\lambda} \tag{6}$$

Here σ_{at} = 100 kN/m^2 is a reference (atmospheric) stress and σ_m is the current mean principal stress in the considered soil element. The parameter κ determines the soil stiffness at the reference stress state and the parameter λ rules the stress dependency of the soil stiffness. The material parameters used here are given in Table 3.

Table 3. Material parameters used for medium dense sand.

Unit buoyant weight γ'	11.0 kN/m^3
Oedometric stiffness parameter κ	600
Oedometric stiffness parameter λ	0.55
Poisson's ratio ν	0.25
Internal friction angle φ'	35.0°
Dilation angle ψ	5.0°
Cohesion c'	0.1 kN/m^2

4.3 Contact Behavior

For the contact behavior of the surface between pile (rigid body) and soil an elasto-plastic model was used. The maximum frictional shear stress $\tau_{fric,max}$ is dependent on the normal stress σ_n and a coefficient of friction μ. In the numerical simulations presented here $\mu = 0.431$ was assumed ($\mu = tan\ (2/3\varphi)$). In order to describe the frictional behavior between the pile and the surrounding soil realistically, the maximum frictional shear stress was limited to a value of 80 kN/m^2, which is approximately the value for medium dense sand recommended in the API design guidelines (API 2000).

For full mobilization of the limit frictional stress the relative displacement (elastic slip) between the pile and the surrounding soil was set to $\Delta u_{el,slip}$ = 0.005 m. The stiffness of the contact (k_τ) before reaching the maximum frictional stress is thus defined as shown in Fig. 4.

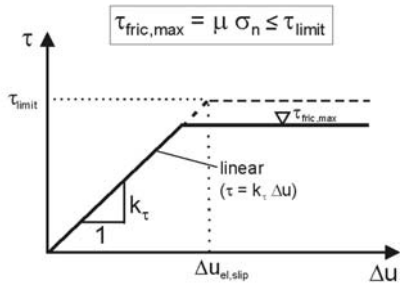

Figure 4. Modeling of contact behavior

4.4 Modeling Procedure

The numerical modeling was performed in three stages. In the first stage the static pull-out capacity of the pile was calculated by increasing the tensile load until failure occurred. In a second stage a certain tensile load – in the investigations presented about 40% of the static pull-out capacity – was applied and the resulting stress-strain behavior of the system was assessed. In a third stage, the volume compactions determined from the results of the second stage and for a certain number of load cycles were applied to the pile-soil system and subsequently the pile load was increased to failure in order to obtain remaining pile capacity after cyclic loading.

The first step was the initialization of geostatic stresses in the soil mass by activating the soil's weight. Afterwards, the soil elements located at the pile position were removed and replaced by the rigid pile body and the contact conditions were activated. In the first stage calculation, the static pile capacity was determined subsequently.

In the second stage calculation, the initial shear strains in the soil elements γ_0 were calculated. As a measure of shear strain, the value proposed by Wegener & Herle (2010) was used:

$$\gamma = \left(\frac{2}{3}\right)^{0.5} \cdot \{(\varepsilon_1 - \varepsilon_2)^2 + (\varepsilon_2 - \varepsilon_3)^2 + (\varepsilon_3 - \varepsilon_1)^2\}^{0.5} \quad (7)$$

Then the cyclic load portion was applied and the shear strains in all soil elements were assessed again, yielding the values γ_1. Using Eq. (7), the volumetric strain for each soil element was determined. For elements in which the cyclic shear strain was smaller than the threshold value $\alpha\ \gamma_{lim}$, the volumetric strain was set to zero. In the calculations presented here, $\alpha\ \gamma_{lim}=5\cdot10^{-5}$ was used.

In the third stage, the degradation behavior under cyclic loading was modeled as follows:

i) To apply the volumetric strain to the pile-soil system, a temperature field was established and applied to the system. The temperature difference and the respective material parameter (temperature expansion coefficient) were chosen such that the resulting shrinkage of an element was identical to the demanded volumetric compaction.

ii) The application of the temperature fields induces stress redistribution in the systems. Thus, the reduction of normal stress acting on the pile is obtained directly by the model.

iii) Finally, the pile was pulled out and the post-cyclic pile capacity was determined.

The steps ii) and iii) were repeated to simulate different number of load cycles (here ranging from 10 to 10,000).

5. Numerical Results

In this study, first results regarding the stress changes in sand soil due to cyclic axial (tensile) pile loading and the resulting post-cyclic pile capacities are presented. In order to investigate the effect of cyclic loading, the number of load cycles was varied from N=1 (static loading) until N=10,000.

Rigid piles in medium dense sand with the parameters given in Table 3 were considered. For this first approach, no distinction was made between soil stiffness values under first time loading and reloading.

5.1 Post-cyclic pile capacity

In Fig. 5 the post-cyclic load-displacement relationships for two different pile geometries are shown. Once a pile with diameter D=2m and length L=30m and once a pile with D=3m and L=20m was considered.

Static pullout-capacities of about 5.75 MN (D=2m, L=30m) and 3.75 MN (D=3m, L=20m) were obtained. The considered cyclic loads were pure swell-loads with a magnitude of 40% of the obtained static capacities. Assessing the volume compaction dependent on the calculated shear strains and the number of load cycles, these values were applied to the model and afterwards pullout was modeled.

As to be expected, a decrease of post-cyclic capacity with the number of load cycles was obtained and can be seen in absolute values in Fig. 5 and as a degradation factor dependent on number of load cycles in Fig. 6. Since the dependence of the volume compaction on the number of load cycles is assumed to be logarithmic, also the decrease of post-cyclic capacity depends on the logarithm of load cycles. Very similar degradation factors were found for the two cases considered. The factors vary from about 7% for N=10 until about 28% for N=10,000. Similar results were also obtained with other pile dimensions. Thus, the results are valid for almost rigid piles with lengths of 20m to 30m under a cyclic swell load of 40% of the static pile capacity.

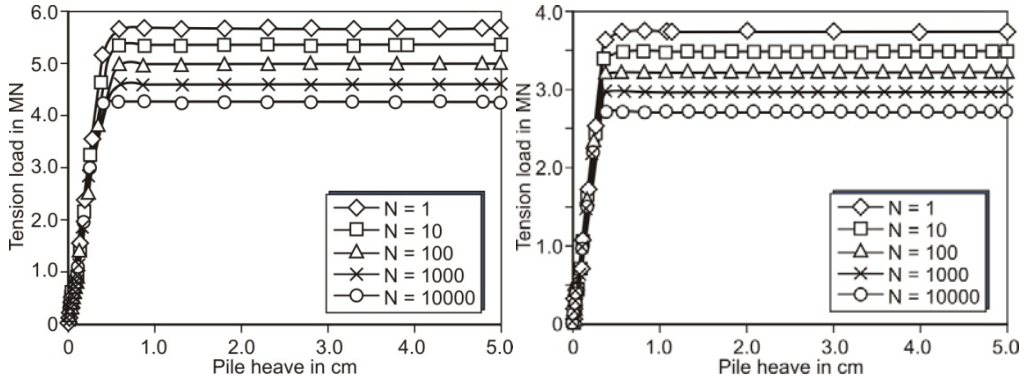

Figure 5. Numerically obtained post-cyclic tensile pile capacities (left: *D*=2m, *L*=30m, right: *D*=3m, *L*=20m)

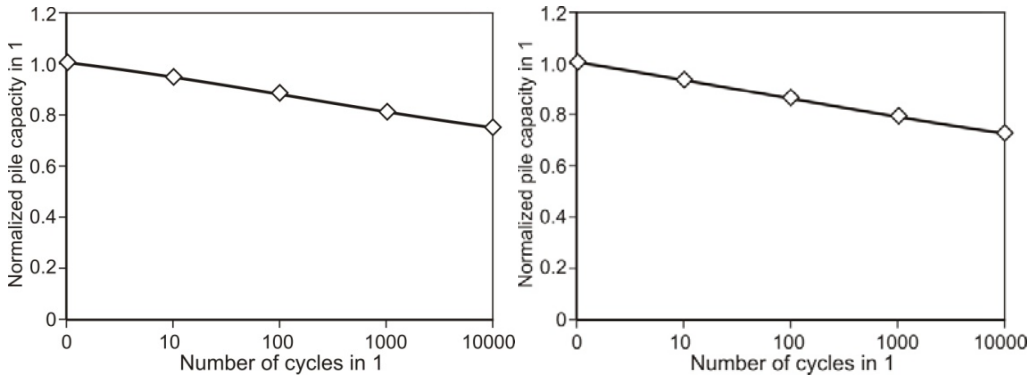

Figure 6. Pile capacity degradation due to cyclic pre-loading (left: *D*=2m, *L*=30m, right: *D*=3m, *L*=20m)

5.2 Skin Friction Degradation

The decrease of the horizontal stress ($\Delta\sigma_h = \Delta\sigma_{11}$) around a pile with a diameter D=2.5m and length L=25m after 100 cycles is shown in Figure 7. The contour plot shows the effect of the cyclic loading on the horizontal stress and consequently on the ultimate skin friction between the pile and the soil. A decrease occurs up to a certain distance from the pile, which is consistent with the theoretical assumptions. This decrease of the horizontal stress is mainly concentrated in the soil beneath the lower part of the pile.

Figure 8 shows the distribution of ultimate skin frictions along the piles after different numbers of load cycles. For the rigid piles in sand considered here, a triangular distribution of ultimate skin friction is obtained for static load condition, as it also can be found in design guidelines (e.g. API 2000). Fig. 8 shows that after cyclic pre-loading this linear distribution changes to a non-linear distribution. The larger the depth, the larger the skin friction degradation becomes. In the first upper meters there is almost no degradation in the skin friction, because the cyclic shear strains in these depths are smaller than the threshold value above which volume compaction occurs. But below, the degradation starts and becomes maximal at the pile tip. This result is valid for rigid piles in homogeneous soil, since here the actual skin friction monotonically increases with depth and thus also the cyclic shear strain amplitudes become larger with depth.

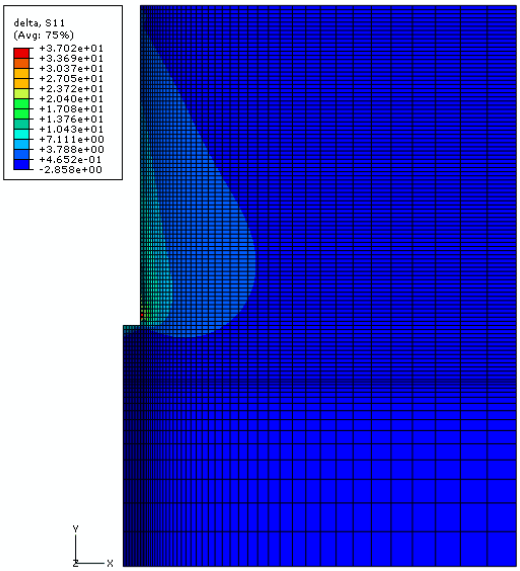

Figure 7. Decrease of the horizontal stress under cyclic loading (D=2.50, L=25.0m, N=100)

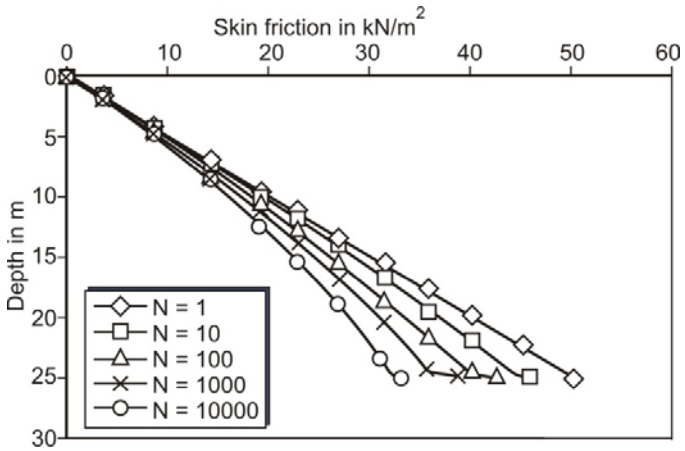

Figure 8. Skin friction degradation under cyclic loading (D=2.50, L=25.0m)

6. Conclusions

A numerical method was developed which is capable to assess stress changes in the soil around a pile due to cyclic axial loading and to figure out the post-cyclic pullout-capacity of the pile with respect to the magnitude of cyclic axial load and the number of load cycles. The method is a numerical realization of an analytical approach of Richter & Kirsch (2010). Here, the volume compaction due to cyclic shearing is assessed empirically dependent on the cyclic shear strains and is then applied to the pile-soil system.

In the paper in hand, mainly the idea and the way of realization of the method are described. First results for rigid piles in homogeneous medium dense sand are presented. The method gives a prediction of post-cyclic pile capacities and is thus a promising tool to assess cyclic load effects on the behavior of axially loaded piles.

In subsequent investigations, further parametric studies will be carried out with non-rigid piles, different relative densities of the sand soil, layered soils and different cyclic load magnitudes. A further refinement of the method is also highly desirable. In particular, consideration of small strain stiffness effects and distinction between first time loading and cyclic un- and reloading is foreseen.

The results presented in this paper were obtained as part of the GIGAWIND ALPHA VENTUS research group project funded by the Federal Ministry for the Environment, Natural Conservation and Nuclear Safety, Germany. The support is thankfully acknowledged.

7. References

1. ABAQUS User's Manual, Version 6.9, Simulia, Providence, RI, USA, 2010.
2. API, "API Recommended Practice 2A-WSD", Recommended Practice for Planning, Designing, Constructing Fixed Offshore Platforms - Working Stress Design; 21st edition, Dallas, 2000.
3. API," Errata and Supplement 3 - API Recommended Practice 2A-WSD", Recommended Practice for Planning, Designing, Constructing Fixed Offshore Platforms - Working Stress Design, 2007.
4. Jardine, E., Standing, "Pile Load Testing Performed for HSE". Cyclic Loading Study at Dunkirk, Volume 1 und 2. In: Offshore Technology Report, HSE Health & Safety Executive, 2000.
5. Kempfert, H.-G., Pfahlgründungen; in: Grundbau-Taschenbuch Teil 3, ed. K.J. Witt, Ernst & Sohn, 2009.
6. Poulos, H.G., "Cyclic Stability Diagram for axially loaded piles". ASCE Journal of Geotechnical Engineering Vol. 114, No. 8, 1988.
7. H. Randolph, M., "Mechanical behaviour of soils under environmentally induced cyclic loads". Lecture at the International Centre for Mechanical Sciences (CISM), Udine, 2009.

8. Richter, T., F. Kirsch ,“Ein analytisch-empirischer Ansatz zur Bestimmung der Tragfähigkeit und der Verformungen von axial zyklisch belasteten Pfählen“. Workshop Offshore-Gründungen von Windkraftanlagen, Karlsruhe, 2010.

9. Schwarz, P., “Beitrag zum Tragverhalten von Verpresspfählen mit kleinem Durchmesser unter axialer zyklischer Belastung“. Lehrstuhl und Prüfamt für Bodenmechanik und Felsmechanik der Technischen Universität München, Schriftenreihe Heft 33, 2002.

10. Silver, L., B. Seed, “Volume Changes in Sands during Cyclic Loading”. In: Proceedings of the American Society of Civil Engineers, Vol. 97, No. SM9,1171-1182, 1971.

11. Wegener, D., I. Herle, “Zur Ermittlung von Scherdehnungen unterhalb von dynamisch belasteten Flächen”, Geotechnik, Vol. 33, No. 1., 12-18, 2010.

12. Vucetic, M. , “Cyclic Threshold Shear Strains in Soils“, Journal of Geotechnical Engineering, Vol. 120, No.12, 2208-2228, 1994.